Electronic Supplementary Material (ESI) for Journal of Materials Chemistry A.
This journal is © The Royal Society of Chemistry 2017

Supporting Information

Electrospun $WNb_{12}O_{33}$ Nanowires: Superior Lithium Storage Capability and Its Working Mechanism

*Lei Yan, Hua Lan, Haoxiang Yu, Shangshu Qian, Xing Cheng, Nengbing Long, Ruifeng Zhang, Miao Shui, Jie Shu**

Faculty of Materials Science and Chemical Engineering, Ningbo University, Ningbo 315211, Zhejiang, China

* Corresponding author: Jie Shu

E-mail: sergio_shu@hotmail.com

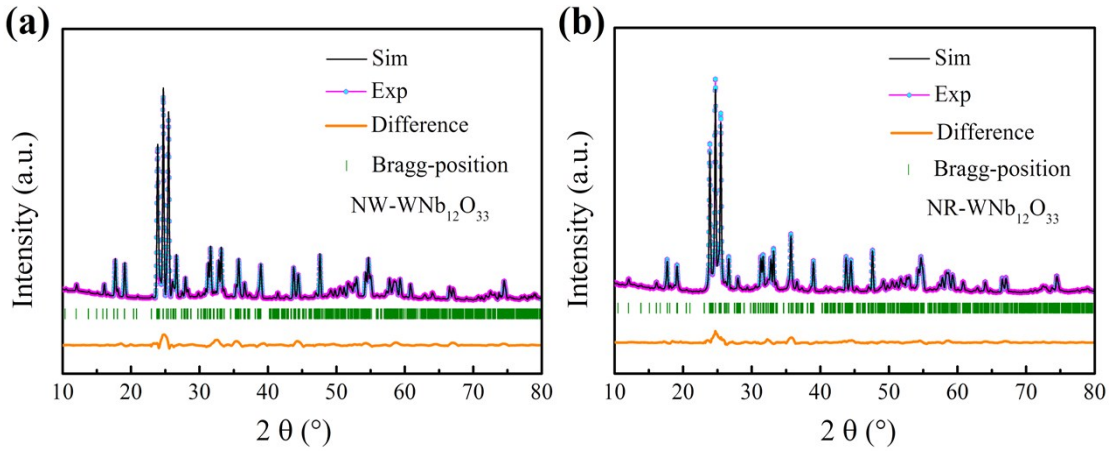

Figure S1. XRD Rietveld refinement profiles of (a) NW-$WNb_{12}O_{33}$ and (b) NR-$WNb_{12}O_{33}$.

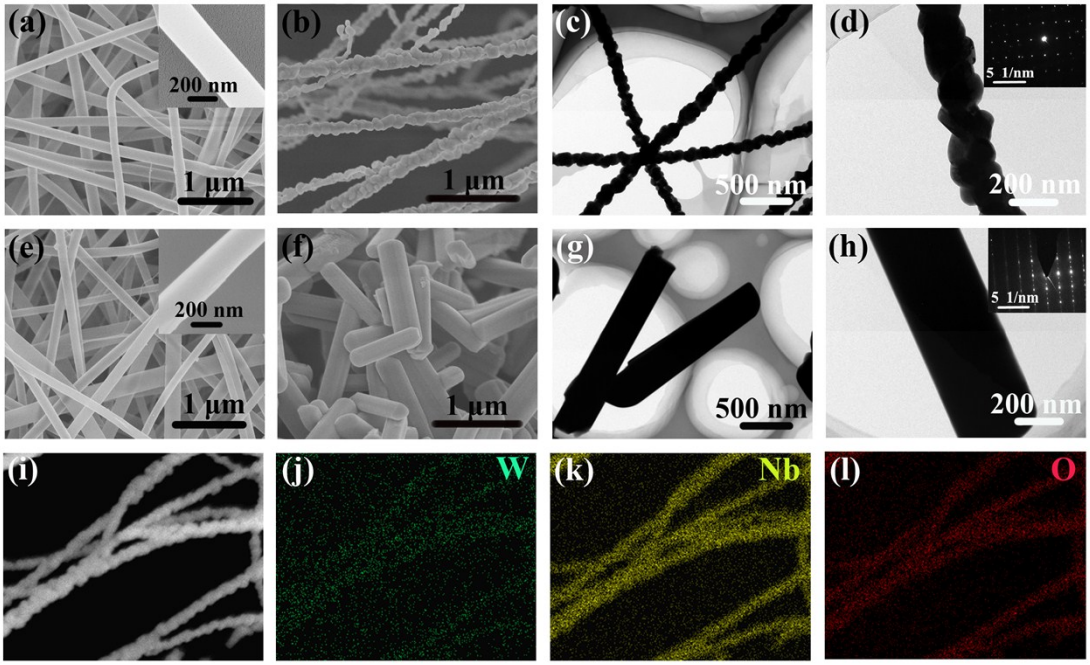

Figure S2. SEM images of precursor nanofibers for (a) NW-$WNb_{12}O_{33}$ and (e) NR-$WNb_{12}O_{33}$, SEM, TEM and SAED images of (b, c, d) NW-$WNb_{12}O_{33}$ and (f, g, h) NR-$WNb_{12}O_{33}$, (b, c, e, f) TEM images of NW-$WNb_{12}O_{33}$ and NR-$WNb_{12}O_{33}$, (i, j, k, l) SEM and EDS elemental mapping images of W, Nb, O elements in NW-$WNb_{12}O_{33}$.

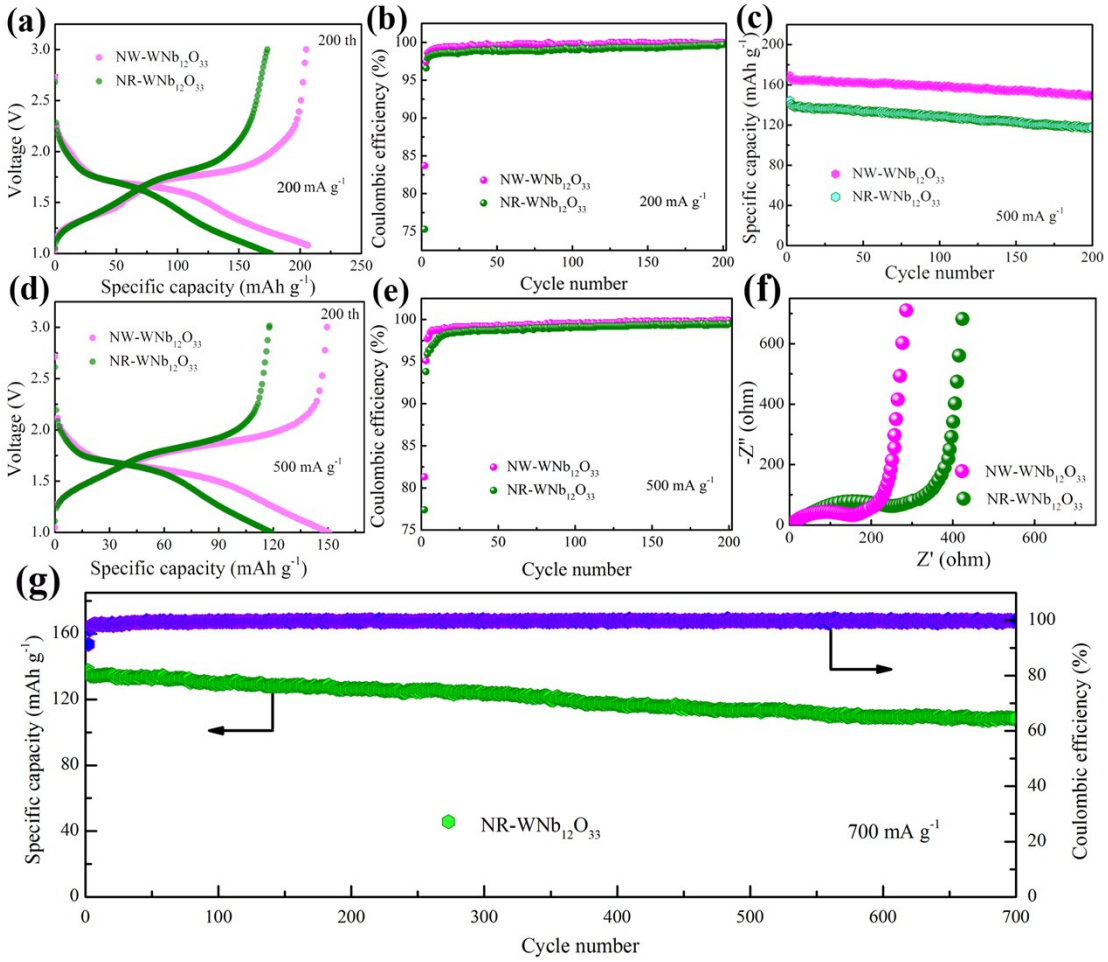

Figure S3. (a, d) The charge/discharge curves after 200 cycles, (b, e) Coulombic efficiencies (c) cycle properties, (f) EIS patterns of NW-$WNb_{12}O_{33}$ and NR-$WNb_{12}O_{33}$. (g) The long-term cycling performance of NR-$WNb_{12}O_{33}$ tested at a high current density of 700 mA g^{-1}.

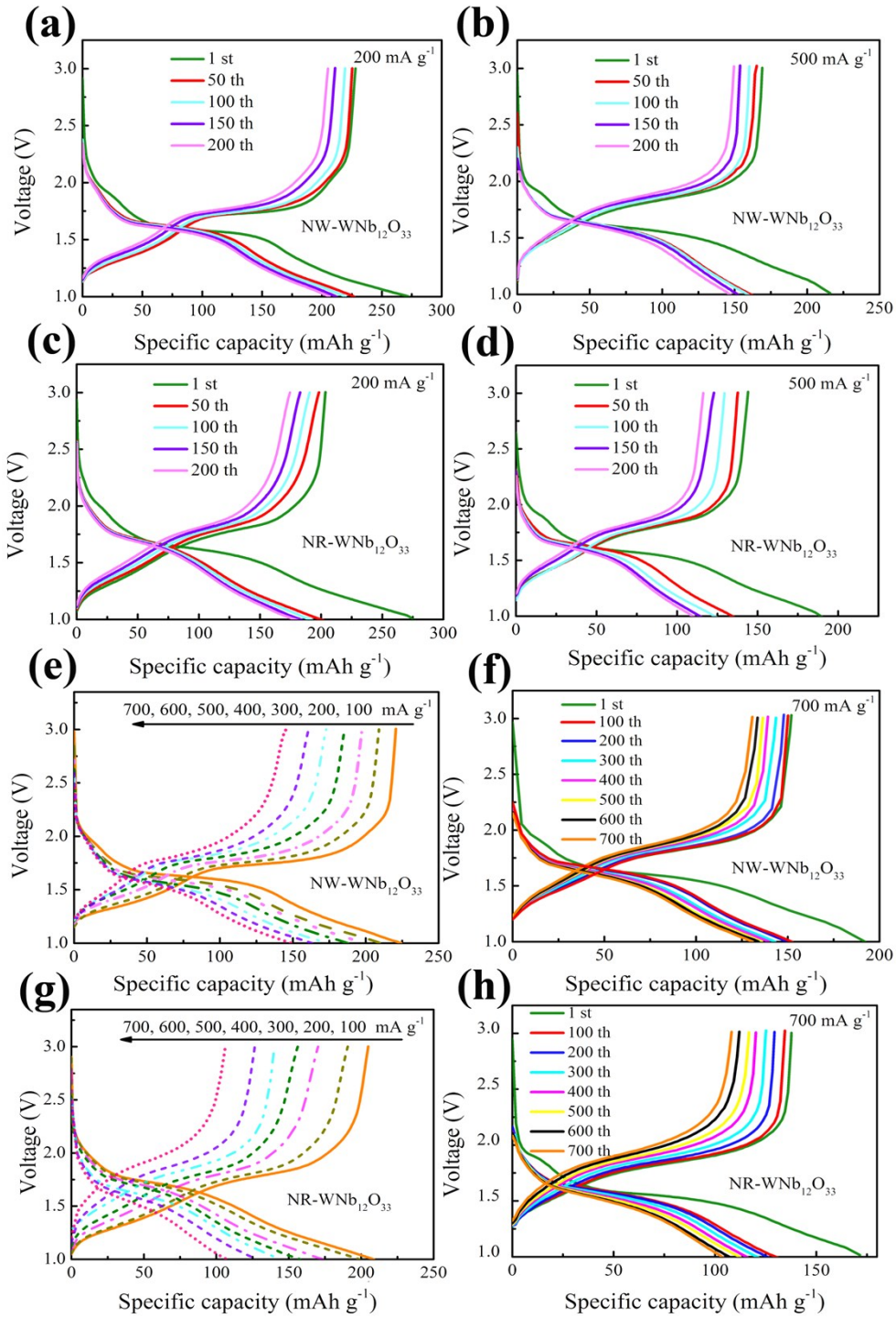

Figure S4. (a, b, f) The galvanostatic charge/discharge voltage profiles of NW-$WNb_{12}O_{33}$ at 200, 500 and 700 mA g^{-1}, respectively. (c, d, h) The galvanostatic charge/discharge voltage profiles of NR-$WNb_{12}O_{33}$ at 200, 500 and 700 mA g^{-1}, respectively. (e, g) The galvanostatic charge/discharge voltage profiles of NW-$WNb_{12}O_{33}$ and NR-$WNb_{12}O_{33}$ at various current densities, respectively.

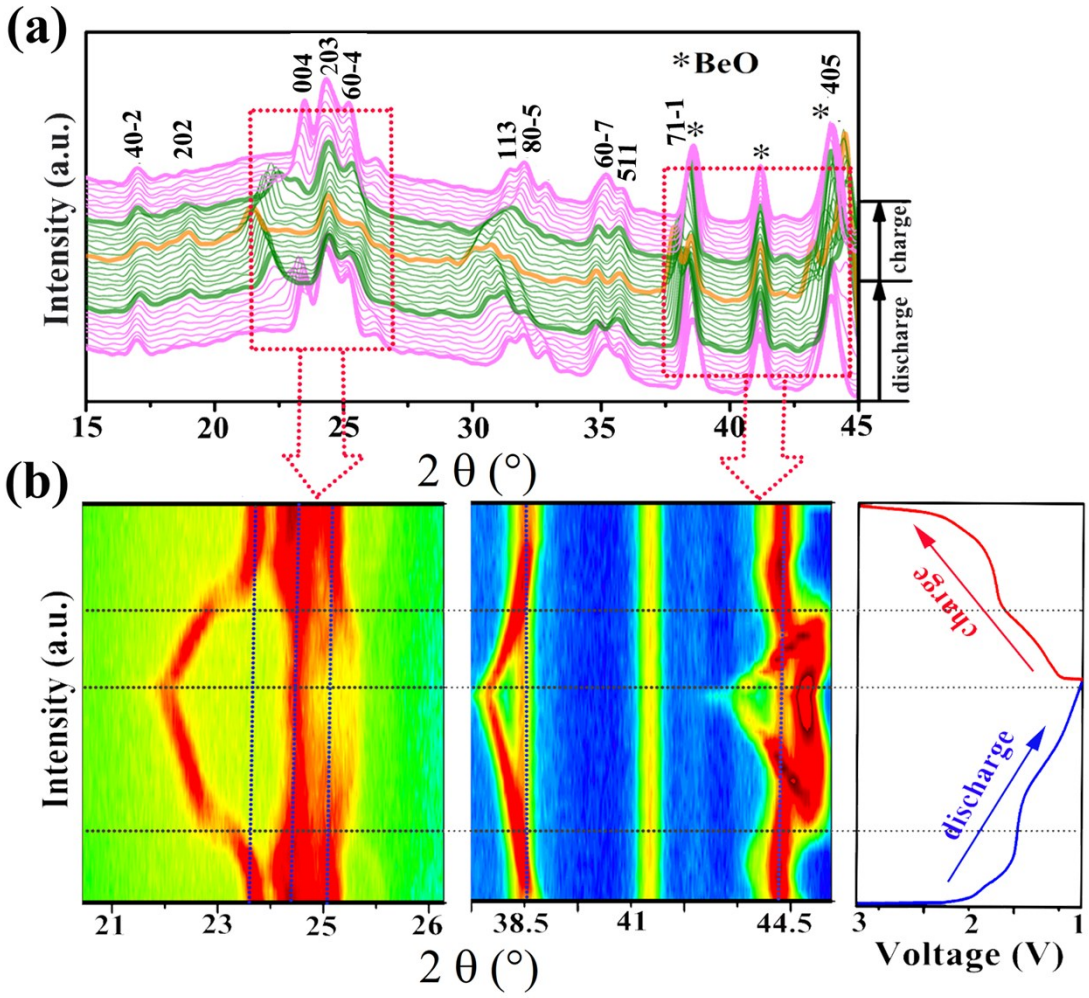

Figure S5. (a) Overall in-situ XRD patterns of NW-$WNb_{12}O_{33}$ during the first discharge/charge process, and (b) corresponding in-situ evolution of relative intensity.

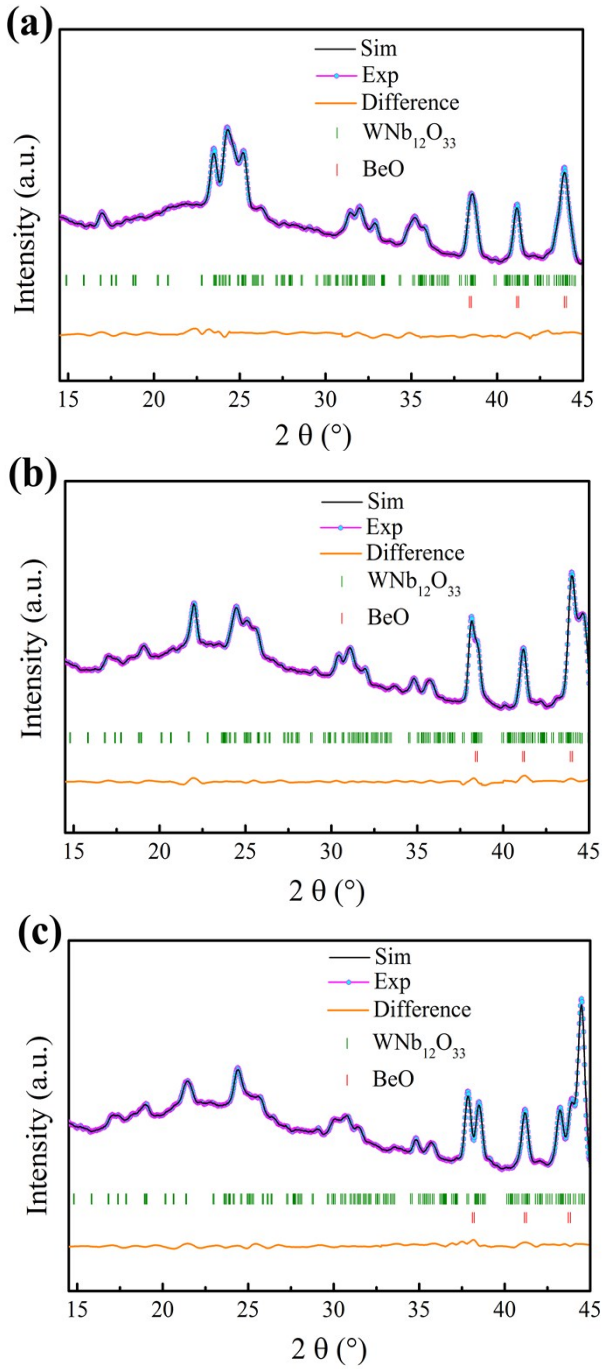

Figure S6. Rietveld refinement patterns for NW-$WNb_{12}O_{33}$ (a) before lithiation, (b) with 4c positions partly occupied by lithium ions during the lithiation process, and (c) with 4c positions fully occupied by lithium ions during the lithiation process.

Table S1. Rietveld refinement data obtained for NW-$WNb_{12}O_{33}$.

Site	Atom	x	y	z	Occupancy
a=22.2474 Å, b=3.8201 Å, c=17.7290 Å, R_p=5.75%, R_{wp}=7.60%					
2a	W	0	0.25000	0	0.08
4c	Nb(1)	0.36630	0	0.04230	0.02
4c	Nb(2)	0.24750	0	0.13580	0.02
4c	Nb(3)	0.12820	0	0.22980	0.01
4c	Nb(4)	0.41650	0	0.37930	0.01
4c	Nb(5)	0.29570	0	0.47150	0.01
4c	Nb(6)	0.46190	0	0.71220	0.02
2b	O(1)	0	0.50000	0.50000	0.02
4c	O(2)	0.15730	0	0.01470	0.01
4c	O(3)	0.30510	0	0.08360	1.00
4c	O(4)	0.03240	0	0.09370	0.08
4c	O(5)	0.45540	0	0.15830	0.39
4c	O(6)	0.18360	0	0.17890	0.43
4c	O(7)	0.05630	0	0.25690	0.01
4c	O(8)	0.33210	0	0.25720	0.97
4c	O(9)	0.47200	0	0.32470	0.08
4c	O(10)	0.20800	0	0.34980	0.03
4c	O(11)	0.35720	0	0.42940	0.02
4c	O(12)	0.23840	0	0.51880	0.01

4c	O(13)	0.37890	0	0.59370	0.05
4c	O(14)	0.08350	0	0.62070	0.05
4c	O(15)	0.40700	0	0.75700	0.05
4c	O(16)	0.29360	0	0.92170	0.03
4c	O(17)	0.43200	0	0.98670	0.09

Table S2. Rietveld refinement data obtained for NR-$WNb_{12}O_{33}$.

Site	Atom	x	y	z	Occupancy
a=22.4973 Å, b=3.8174 Å, c=17.7263 Å, R_p=9.42%, R_{wp}=11.50%					
2a	W	0	0.25000	0	0.08
4c	Nb(1)	0.36630	0	0.04230	0.02
4c	Nb(2)	0.24750	0	0.13580	0.02
4c	Nb(3)	0.12820	0	0.22980	0.01
4c	Nb(4)	0.41650	0	0.37930	0.01
4c	Nb(5)	0.29570	0	0.47150	0.01
4c	Nb(6)	0.46190	0	0.71220	0.02
2b	O(1)	0	0.50000	0.50000	0.02
4c	O(2)	0.15730	0	0.01470	0.01
4c	O(3)	0.30510	0	0.08360	1.00
4c	O(4)	0.03240	0	0.09370	0.08
4c	O(5)	0.45540	0	0.15830	0.38
4c	O(6)	0.18360	0	0.17890	0.43
4c	O(7)	0.05630	0	0.25690	0.01
4c	O(8)	0.33210	0	0.25720	0.95
4c	O(9)	0.47200	0	0.32470	0.08
4c	O(10)	0.20800	0	0.34980	0.03
4c	O(11)	0.35720	0	0.42940	0.02
4c	O(12)	0.23840	0	0.51880	0.01

4c	O(13)	0.37890	0	0.59370	0.05
4c	O(14)	0.08350	0	0.62070	0.05
4c	O(15)	0.40700	0	0.75700	0.05
4c	O(16)	0.29360	0	0.92170	0.03
4c	O(17)	0.43200	0	0.98670	0.09

Table S3. A comparison of the rate performances between $WNb_{12}O_{33}$ and the reported anode materials.

Samples	Reversible capacity (mAh g^{-1})						
	0.5 C	**1.0 C**	**2.0 C**	**3.0 C**	**4.0 C**	**5.0 C**	**6.0 C**
$WNb_{12}O_{33}$ nanowires	220.8	209.1	197.2	184.4	172.9	159.8	145.7
$WNb_{12}O_{33}$ nanorods	204.8	190.7	170.1	155.9	143.7	125.9	105.7
Nb_2O_5 nanowires [51]	180	160	153	146	139	128	115
Nb_2O_5 microspheres [49]	-	151	-	140	-	122	113
Nb_2O_5 nanosheets [52]	-	160	135	-	-	90	-
Nb_2O_5@C nanocomposites [53]	150	130	-	-	90	-	-
$Ti_2Nb_{10}O_{29}$ particles [54]	221	210	190	-	-	125	-
C-$FeNbO_4$ particles [55]	99.24	85.08	-	-	-	-	-

Table S4. Rietveld refinement data for NW-$WNb_{12}O_{33}$ before lithiation.

Site	Atom	x	y	z	Occupancy
a=22.2851 Å, b=3.8527 Å, c=17.7628 Å, R_p=1.99%, R_{wp}=2.63%					
2a	W	0	0.25000	0	0.08
4c	Nb(1)	0.36630	0	0.04230	0.02
4c	Nb(2)	0.24750	0	0.13580	0.02
4c	Nb(3)	0.12820	0	0.22980	0.01
4c	Nb(4)	0.41650	0	0.37930	0.01
4c	Nb(5)	0.29570	0	0.47150	0.01
4c	Nb(6)	0.46190	0	0.71220	0.02
2b	O(1)	0	0.50000	0.50000	0.02
4c	O(2)	0.15730	0	0.01470	0.01
4c	O(3)	0.30510	0	0.08360	1.00
4c	O(4)	0.03240	0	0.09370	0.08
4c	O(5)	0.45540	0	0.15830	0.37
4c	O(6)	0.18360	0	0.17890	0.42
4c	O(7)	0.05630	0	0.25690	0.01
4c	O(8)	0.33210	0	0.25720	0.97
4c	O(9)	0.47200	0	0.32470	0.08
4c	O(10)	0.20800	0	0.34980	0.03
4c	O(11)	0.35720	0	0.42940	0.02
4c	O(12)	0.23840	0	0.51880	0.01

4c	O(13)	0.37890	0	0.59370	0.05
4c	O(14)	0.08350	0	0.62070	0.05
4c	O(15)	0.40700	0	0.75700	0.05
4c	O(16)	0.29360	0	0.92170	0.03
4c	O(17)	0.43200	0	0.98670	0.09

Table S5. Rietveld refinement data for NW-$WNb_{12}O_{33}$ with 4c positions partly occupied by lithium ions during the lithiation process.

Site	Atom	x	y	z	Occupancy
a=22.3731 Å, b=3.8292 Å, c=17.8764 Å, R_p=2.06%, R_{wp}=2.86%					
2a	W	0	0.25000	0	0.08
4c	Nb(1)	0.36630	0	0.04230	0.02
4c	Nb(2)	0.24750	0	0.13580	0.02
4c	Nb(3)	0.12820	0	0.22980	0.01
4c	Nb(4)	0.41650	0	0.37930	0.01
4c	Nb(5)	0.29570	0	0.47150	0.01
4c	Nb(6)	0.46190	0	0.71220	0.02
2b	O(1)	0	0.50000	0.50000	0.02
4c	O(2)	0.15730	0	0.01470	0.01
4c	O(3)	0.30510	0	0.08360	1.00
4c	O(4)	0.03240	0	0.09370	0.08
4c	O(5)	0.45540	0	0.15830	0.37
4c	O(6)	0.18360	0	0.17890	0.43
4c	O(7)	0.05630	0	0.25690	0.01
4c	O(8)	0.33210	0	0.25720	0.96
4c	O(9)	0.47200	0	0.32470	0.08
4c	O(10)	0.20800	0	0.34980	0.03
4c	O(11)	0.35720	0	0.42940	0.02

4c	O(12)	0.23840	0	0.51880	0.01
4c	O(13)	0.37890	0	0.59370	0.05
4c	O(14)	0.08350	0	0.62070	0.05
4c	O(15)	0.40700	0	0.75700	0.05
4c	O(16)	0.29360	0	0.92170	0.03
4c	O(17)	0.43200	0	0.98670	0.09
4c	Li(1)	0.06380	1.00000	0.44820	0.09
4c	Li(2)	0.73830	0.50000	0.69890	0.36

Table S6. Rietveld refinement data for NW-$WNb_{12}O_{33}$ with 4c positions fully occupied by lithium ions during the lithiation process.

Site	Atom	x	y	z	Occupancy
a=22.3530 Å, b=3.8345 Å, c=17.8647 Å, R_p=2.15%, R_{wp}=3.09%					
2a	W	0	0.25000	0	0.08
4c	Nb(1)	0.36630	0	0.04230	0.02
4c	Nb(2)	0.24750	0	0.13580	0.02
4c	Nb(3)	0.12820	0	0.22980	0.01
4c	Nb(4)	0.41650	0	0.37930	0.01
4c	Nb(5)	0.29570	0	0.47150	0.01
4c	Nb(6)	0.46190	0	0.71220	0.02
2b	O(1)	0	0.50000	0.50000	0.02
4c	O(2)	0.15730	0	0.01470	0.01
4c	O(3)	0.30510	0	0.08360	1.00
4c	O(4)	0.03240	0	0.09370	0.08
4c	O(5)	0.45540	0	0.15830	0.38
4c	O(6)	0.18360	0	0.17890	0.44
4c	O(7)	0.05630	0	0.25690	0.01
4c	O(8)	0.33210	0	0.25720	0.96
4c	O(9)	0.47200	0	0.32470	0.08
4c	O(10)	0.20800	0	0.34980	0.03
4c	O(11)	0.35720	0	0.42940	0.02

4c	O(12)	0.23840	0	0.51880	0.01
4c	O(13)	0.37890	0	0.59370	0.05
4c	O(14)	0.08350	0	0.62070	0.05
4c	O(15)	0.40700	0	0.75700	0.05
4c	O(16)	0.29360	0	0.92170	0.03
4c	O(17)	0.43200	0	0.98670	0.09
4c	Li(1)	0.06380	1.00000	0.44820	0.09
4c	Li(2)	0.73830	0.50000	0.69890	0.35
4c	Li(3)	0.88750	1.00000	0.19560	0